PROBLEMY MECHATRONIKI
UZBROJENIE, LOTNICTWO, INŻYNIERIA BEZPIECZEŃSTWA

ISSN 2081-5891

9, 4 (34), 2018, 149-162

PROBLEMS OF MECHATRONICS
ARMAMENT, AVIATION, SAFETY ENGINEERING

An Application of a Special Method for Designating the Control Forces for the Homing of an Anti-Aircraft Missile on an Aerial Target by Use of a Method of Proportional Navigation

Konrad STEFAŃSKI

Kielce University of Technology, Faculty of Mechatronics and Mechanical Engineering,
7 Tysiąclecia Państwa Polskiego Av., 25-314 Kielce, Poland
E-mail address: stefan5@interia.pl

Received by the editorial staff on 7 June 2016
The reviewed and verified version was received on 18 December 2018

DOI 10.5604/01.3001.0012.7339

Abstract. An analysis of application feasibility of a special method for surface-to-air missile (SAM) control during homing on an airborne target was carried out in this paper. A prior implementation of the method was motion control for a gyroscope axis with three degrees of freedom [1, 2] at the stages of spatial seeking and tracking of a detected target. The positive results obtained during that research led to a conclusion that the proposed control method would be appropriate for the determination of the control forces for missile guidance. This method consists in the application of the phase trajectories of control errors. Switching over of the control forces at suitable phase plane points reduced the control errors to zero and facilitated a proper flight path of the SAM. This paper presents a switching algorithm, equations of the kinematics and dynamics of SAM flight, and a number of examples of numerical simulations of the problem contemplated herein. The simulation results were represented in a graphic format.
Keywords: mechanics, control, phase trajectories, homing, target

1. INTRODUCTION

The selection of the control system and the guidance method of surface-to-air missiles (SAMs) to facilitate a SAM's interception of a moving airborne target is one of the most important problems in studies of SAM flight. The problem explicitly implies that a SAM flight path must be chosen as determined by the SAM's guidance algorithm. A guidance algorithm should be selected so that a number of conditions are satisfied, including small gravity loads, ease of homing performance, and the method of control force determination that is feasible in real-world conditions. A SAM can be controlled in two ways that can be combined and implemented together: aerodynamic control and gas-dynamic control [3]. It is also important to properly identify the initial launch conditions of a SAM which largely affect the curve of the SAM's flight path. The solution to this problem is often very complex and only viable with numerical methods. This is due to the complex equations of the flight dynamics of SAMs, including the control circuit dynamics, control actuator dynamics, and much more. The control factor of a SAM is the control forces Q_y and Q_z. In computer simulations, the control forces emulate the lift from the air sweeping the control surfaces of the SAM in flight [4, 5].

The analysis of the control method proposed in this paper involved the determination and cross-comparison of the desired and actual SAM flight paths, the check and evaluation of the determined control forces essential for target homing of a SAM, the check of the control error values, the check of the total g-load applied to a SAM in mid flight, and a visual representation of the flight angles of a SAM and the target line of sight (T-LOS), and the attack and sideslip angles (or drift) of a SAM. The moving airborne target was attacked by the SAM from the front hemisphere (FH) and the aft hemisphere (AH). The situations are shown in Fig. 1. The SAM as the test object was homed to the airborne target with a method most universal as based on a proportional navigation algorithm. One of the elements of the system which provided target identification and tracking with precise and reliable guidance of the SAM to the airborne target following a correct flight trajectory could be an optical seeker [6, 7]; however, this paper does not consider this topic.

2. EQUATIONS OF SAM MOTION

The equations of the flight kinematic and dynamics of the SAM were derived in the coordinate systems shown in Fig. 2. The figure shows the angles of rotation of the individual reference systems relative to each other.

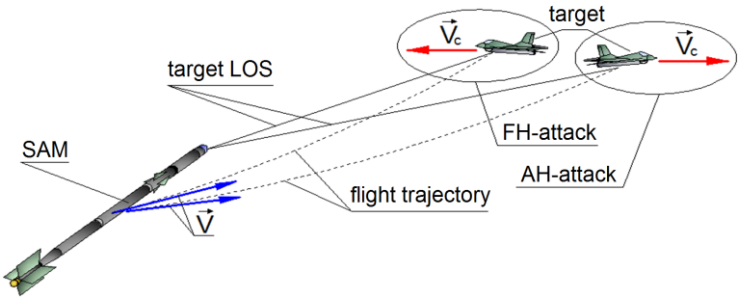

Fig. 1. Cases of airborne target attack by a homing SAM in the front (FH) and aft (AH) hemispheres

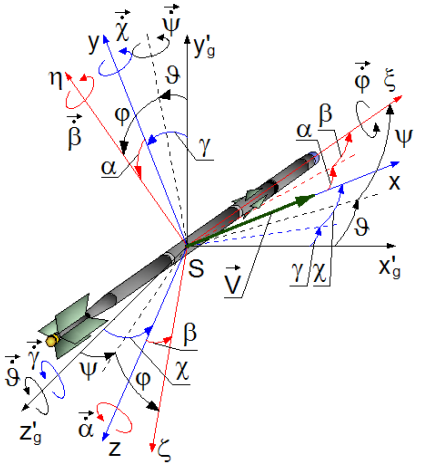

Fig. 2. Coordinate systems and their rotation angles assumed to derive the SAM's equations of flight path

The key to the designations in the foregoing figure follow [8, 9]: $Sx'_g y'_g z'_g$ – coordinate system with the origin at the SAM and parallel to the launch coordinate system; $S\xi\eta\zeta$ – coordinate system related to the SAM and generated by the rotations of the coordinate system $Sx'_g y'_g z'_g$ by angle ϑ, ψ and φ, (which were, respectively: pitch angle, yaw angle and roll angle of the SAM, rad); $Sxyz$ – velocity coordinate system related to the air stream flow and generated by the rotations of the coordinate system $Sx'_g y'_g z'_g$ by angles γ and χ (the SAM flight angles, rad); α, β – respectively: the attack angle and the sideslip angle, rad; $\vec{V}$ – velocity vector of the SAM.

The equations for the kinematic relations between the SAM and its target were [10]:

$$\frac{dr}{dt} = V_c\left[\cos\chi_c\cos\sigma\cos(\varepsilon-\gamma_c)+\sin\chi_c\sin\sigma\right]+ \\ -V\left[\cos\chi\cos\sigma\cos(\varepsilon-\gamma)+\sin\chi\sin\sigma\right] \tag{1}$$

$$r\frac{d\varepsilon}{dt}\cos\sigma = -V_C\cos\chi_C\sin(\varepsilon-\gamma_C)+V\cos\chi\sin(\varepsilon-\gamma) \tag{2}$$

$$-r\frac{d\sigma}{dt}\cos\sigma = V_c\left[\cos\chi_c\sin\sigma\cos(\varepsilon-\gamma_c)\right]+ \\ -V\left[\cos\chi\sin\sigma\cos(\varepsilon-\gamma)-\sin\chi\cos\sigma\right] \tag{3}$$

with: r – SAM's distance to the target, m; V – SAM's velocity, m; V_c – target's velocity, m/s; γ, χ – desired flight angles of the SAM, rad; γ_c, χ_c – pitch and yaw angles of the target velocity vector, rad; ε, σ – pitch and yaw angle of T-LOS, rad.

The SAM was assumed to feature a non-deformable body which did not rotate along its centreline ($\varphi = 0$) and it featured a constant mass [10]. Figure 3 shows a system of forces applied to the SAM during flight.

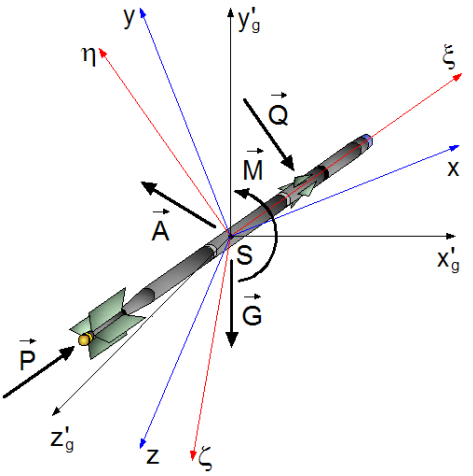

Fig. 3. Forces applied to the SAM

The designations follow: $\vec{G}$ – gravity force vector; $\vec{Q}$ – control force vector; $\vec{M}$ – vector of the total of moments and forces applied to the SAM; $\vec{A}$ – aerodynamic force resultant vector; $\vec{P}$ – rocket motor thrust vector.

The equations of the SAM flight path were expressed as follows [10, 11]:

$$\frac{dV}{dt} = \frac{P}{m}\cos\alpha\cos\beta - g\sin\gamma_r\cos\chi_r - \lambda_x V^2 \tag{4}$$

$$\frac{d\gamma_r}{dt} = \left(\frac{P}{m}\sin\alpha\cos\beta - g\cos\gamma_r + \lambda_y V^2\alpha + \frac{Q_y}{m}\right)\frac{1}{V\cos\chi_r} \tag{5}$$

$$\frac{d\chi_r}{dt} = \frac{P}{mV}\sin\beta + \frac{g}{V}\sin\gamma_r\sin\chi_r - \lambda_z V\beta - \frac{Q_z}{mV} \tag{6}$$

$$\frac{d\omega_\zeta}{dt} = -D_1\frac{V^2}{l}\alpha - D_2 V\frac{d\alpha}{dt} - D_3\frac{d\vartheta}{dt} + \frac{M_z}{J_k} - \left(\frac{J_0}{J_k} - 1\right)\omega_\eta\omega_\xi \tag{7}$$

$$\frac{d\omega_\eta}{dt} = -D_1\frac{V^2}{l}\beta - D_2 V\frac{d\beta}{dt} - D_3 V\frac{d\psi}{dt} + \frac{M_y}{J_k} + \left(\frac{J_0}{J_k} - 1\right)\omega_\zeta\omega_\xi \tag{8}$$

$$\omega_\xi = -\frac{d\vartheta}{dt}\sin\psi, \quad \omega_\eta = \frac{d\psi}{dt}, \quad \omega_\zeta = \frac{d\vartheta}{dt}\cos\psi \tag{9}$$

$$\lambda_x = \frac{\Lambda_x}{m}, \quad \lambda_y = \frac{\Lambda_y}{m}, \quad \lambda_z = \frac{\Lambda_z}{m}, \quad D_{1,2,3} = \frac{C_i l}{J_k} \tag{10}$$

$$\Lambda_x = c_x\frac{\rho}{2}S, \quad \Lambda_y = c_y\frac{\rho}{2}S_y, \quad \Lambda_z = c_z\frac{\rho}{2}S_z \tag{11}$$

with: γ_r, χ_r – realised flight angles of the SAM, rad; m – SAM's mass, kg; l – SAM's body length; J_k, J_0 – primary central moments of inertia of the SAM relative to the SAM's transversal and longitudinal axes, kgm^2; M_y, M_z – SAM's flight control moments, Nm; Q_y, Q_z – SAM's flight control forces, N; ω_ξ, ω_η, ω_ζ – projections of the SAM's body angular velocity vector (the angular velocity vector of the SAM body coordinate system relative to the launch coordinate system) on the related coordinate system's axes, rad/s; g – gravitational acceleration, m/s^2; λ_x, λ_y, λ_z, $D_{1,2,3}$ – relative aerodynamic coefficients of aerodynamic forces and aerodynamic moments, 1/m [10]; ρ – air density, kg/m^3; c_x, c_y, c_z – coefficients of aerodynamic forces; S – surface area of the SAM's cross-section, SAM diameter (calibre) dependent, m^2; S_y, S_z - area of the lifting surface and the drift surface, m^2; C_i – coefficients of aerodynamic force moments; t – time, s.

The attack and sideslip angles of the SAM were determined as follows:

$$\beta = \arcsin\left(\cos\chi_r\sin\psi - \sin\chi_r\cos\psi\cos\left(\vartheta - \gamma_r\right)\right) \tag{12}$$

$$\alpha = \arcsin\left(\frac{\cos\psi \sin(\vartheta - \gamma_r)}{\cos\beta}\right) \tag{13}$$

3. HOMING ALGORITHM AND THE CONTROL FORCES

The SAM was homed with a proportional navigation algorithm which was determined as follows [10, 12]:

$$\frac{d\gamma}{dt} = a_1 \frac{d\varepsilon}{dt}, \ \frac{d\chi}{dt} = a_2 \frac{d\sigma}{dt} \tag{14}$$

with: $a_1 = a_2 = 4$ – proportional navigation constants.

The analysis of the SAM's flight also required the determination of the kinetic g-loads applied to the SAM. The kinetic g-load values were determined with these dependencies [10]:

$$n_x = -\left(\frac{\frac{dV}{dt}}{g} + \sin\gamma_r \cos\chi_r\right), \ n_y = -\left(\frac{V}{g}\frac{d\gamma}{dt}\cos\chi_r + \cos\gamma_r\right) \tag{15a}$$

$$n_z = \frac{V}{g}\frac{d\chi_r}{dt} - \sin\gamma_r \sin\chi_r, \ n = \sqrt{n_x^2 + n_y^2 + n_z^2} \tag{15b}$$

The SAM's control forces were formulated with the method discussed in [1, 2]. The method applied phase trajectories of control errors and reduced the control errors to zero by switching the control forces at suitable phase plane points. The control forces were determined as follows:

$$Q_y = -u_1\left(p_1 \operatorname{sgn} e_{1y} + p_2 \operatorname{sgn} e_{2y} + p_3 \operatorname{sgn} e_{3y}\right) \tag{16a}$$

$$Q_z = -u_2\left(q_1 \operatorname{sgn} e_{1z} + q_2 \operatorname{sgn} e_{2z} + q_3 \operatorname{sgn} e_{3z}\right) \tag{16b}$$

with: $u_{1,2}$, $p_{1,2,3}$, $q_{1,2,3}$ – control factors.

The control errors at $t_0 = 1$, s and t_k, corresponding to the time from the SAM launch to target hit, were determined from the following dependencies:

$$e_{1y} = \gamma - \gamma_r, \ e_{1z} = \chi - \chi_r \tag{17a}$$

$$e_{2y} = \frac{d\gamma}{dt} - \frac{d\gamma_r}{dt}, \ e_{2z} = \frac{d\chi}{dt} - \frac{d\chi_r}{dt} \tag{17b}$$

$$e_{3y} = \int_{t_0}^{t_k} (\gamma - \gamma_r)dt, \ e_{3z} = \int_{t_0}^{t_k} (\chi - \chi_r)dt \tag{17c}$$

The control moments were formulated as follows:

$$M_y = Q_y \cdot e,\ M_z = Q_z \cdot e \tag{18}$$

with: e = 0.7 m – distance between the control force application point and the SAM's centre of mass.

4. COMPUTER SIMULATION RESULTS

The numerical simulations were performed for a hypothetical SAM [13] which attacked its airborne target from FH and AH. The tests were run for the following values:

- SAM's initial velocity: V_0 = 20 m/s;
- target velocity: V_c = *const* =300 m/s;
- SAM's initial position: x_0 = 0 m, y_0 = 0 m, z_0 = 0 m;
- target's initial position for the FH attack: x_{c0} = 5500 m, y_{c0} = 3000 m, z_{c0} = -100 m;
- target's initial position for the AH attack: x_{c0} = 3000 m, y_{c0} = 3000 m, z_{c0} = -100 m;
- SAM's specifications: m = 10.8 kg, l = 1.6 m, J_k = 2.304 kgm^2, J_0 = 0.007 kgm^2; λ_x = 0.000171 1/m, λ_y = λ_z = 0.0051 1/m, D_1 = 0.081 1/m, D_2= 0.0821 1/m, D_3 = 0.00041 1/m, P = 3100 N at $t \in \langle 0,1 \rangle$ s and P = 700 N at t > 1 s.

4.1. The FH attack

In this case, the target was assumed to follow a flight path described with the following equations:

$$\gamma_c(t) = \pi - 0{,}01 \cdot t, \qquad \chi_c(t) = 0{,}1 + 0{,}015 \cdot t \tag{19}$$

The test results for the FH attack were:

- T-LOS pitch angle initial value: ε_0 = 0.4993 rad (28.61 deg);
- T-LOS yaw angle initial value: σ_0 = 0.016 rad (0.91 deg);
- SAM's initial distance to the target: $r_0 = 6.27 \cdot 10^3$ m;
- SAM's target hit accuracy: r_k = 6.25 m;
- time from the SAM launch to the target hit: t_k = 10.18 s;
- values of the control factors: u_1 = -20, u_2 = -8.5, p_1 =q_1 =- 0.75; p_2 =q_2 =- 1, p_3 =q_3 =- 0.75.

The numerical simulation results are shown in a graphical format in Figs. 4 to 13.

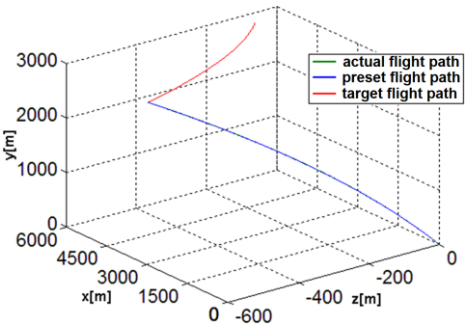

Fig. 4. The SAM and target flight-paths in space

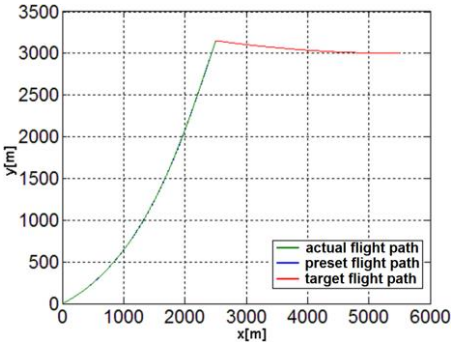

Fig. 5. The SAM and target flight-paths in the vertical plane

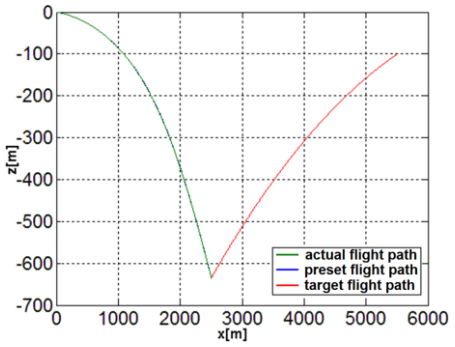

Fig. 6. The SAM and target flight-paths in the horizontal plane

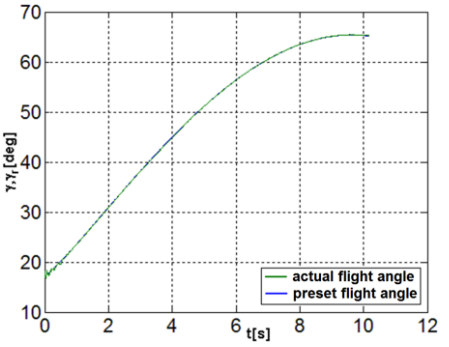

Fig. 7. Desired and actual angles of SAM flight-path in the vertical plane

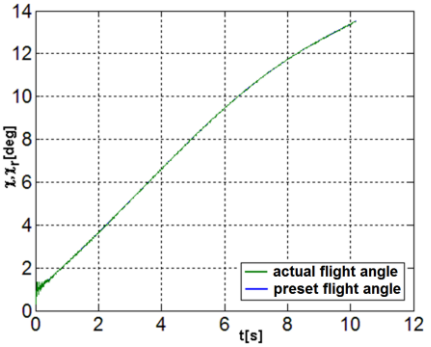

Fig. 8. Desired and actual angles of SAM flight-paths in the horizontal plane

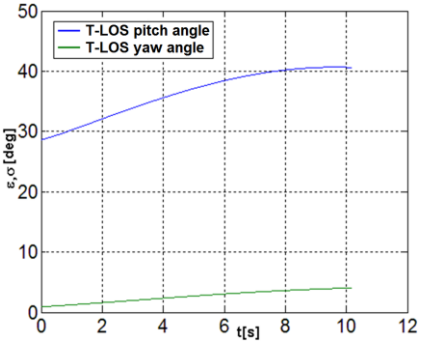

Fig. 9. Values of pitch and yaw angles of the T-LOS

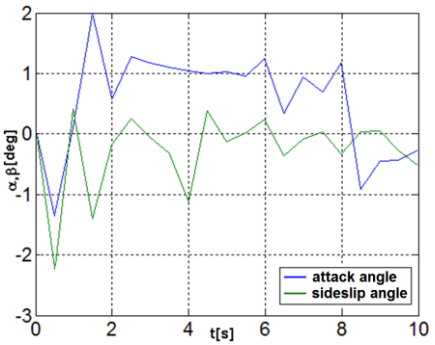

Fig. 10. Attack and sideslip angles

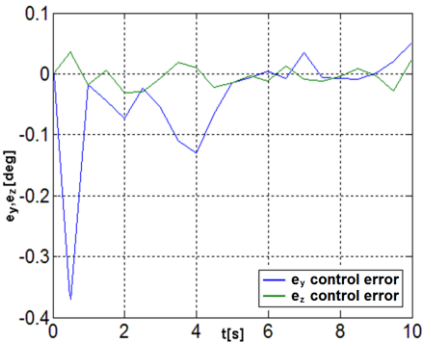

Fig. 11. Control errors

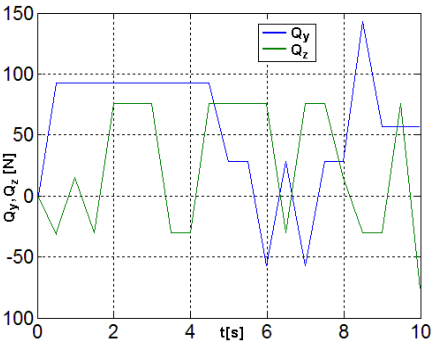

Fig. 12. Control force values

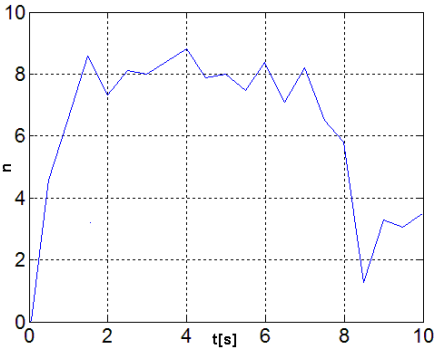

Fig. 13. Kinematic g-loads

4.2. The AH attack

In this case, the target was assumed to follow a flight path described with the following equations:

$$\gamma_c(t) = 0{,}003 \cdot t, \qquad \chi_c(t) = 0{,}045 \cdot t \tag{20}$$

The test results for the AH attack were:

- T-LOS pitch angle initial value: $\varepsilon_0 = 0.7854$ rad (45 deg);
- T-LOS yaw angle initial value: $\sigma_0 = 0.024$ rad (1.35 deg);
- SAM's initial distance to the target: $r_0 = 4.24 \cdot 10^3$ m;
- SAM's target hit accuracy: $r_k = 5.90$ m;
- time from the SAM launch to the target hit: $t_k = 18.16$ s;
- values of the control factors: $u_1 = -15$, $u_2 = -5.5$, $p_1 = q_1 = -0.25$; $p_2 = q_2 = -1$, $p_3 = q_3 = -0.75$.

The numerical simulation results are shown in a graphical format in Figs. 14 to 23.

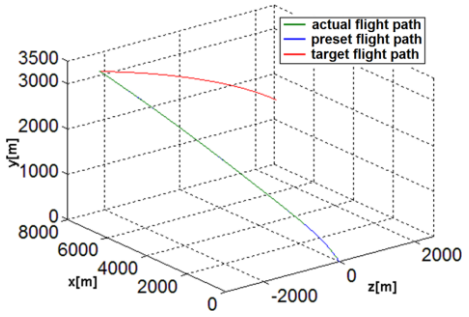

Fig. 14. The SAM and target flight-paths in space

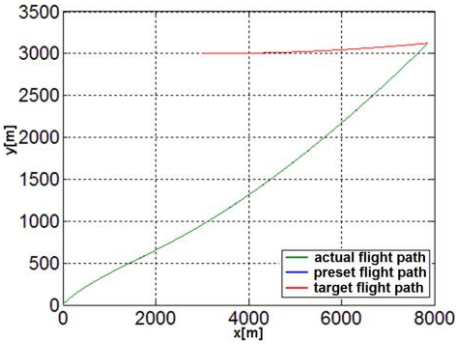

Fig. 15. The SAM and target flight-paths in the vertical plane

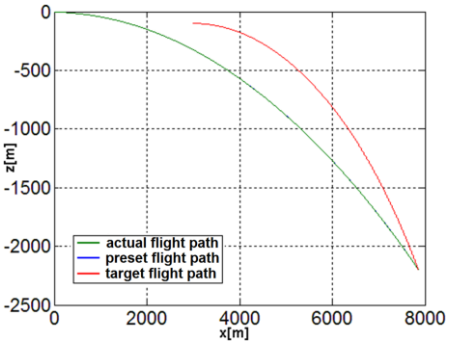

Fig. 16. The SAM and target flight-paths in the horizontal plane

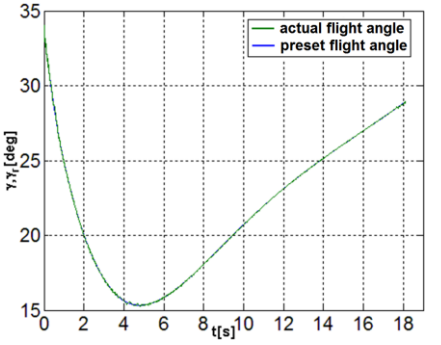

Fig. 17. Desired and actual angles of SAM flight-path in the vertical plane

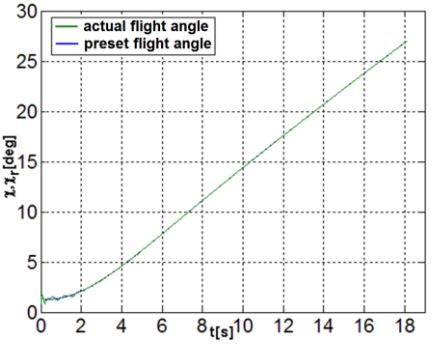

Fig. 18. Desired and actual angles of SAM flight-path in the horizontal plane

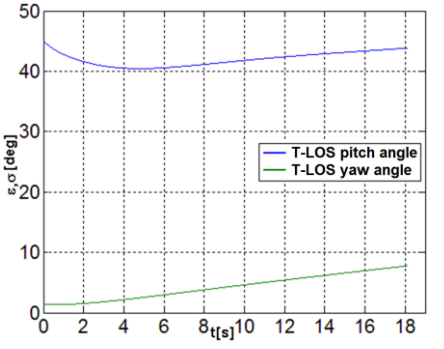

Fig. 19. Values of pitch and yaw angles of the T-LOS

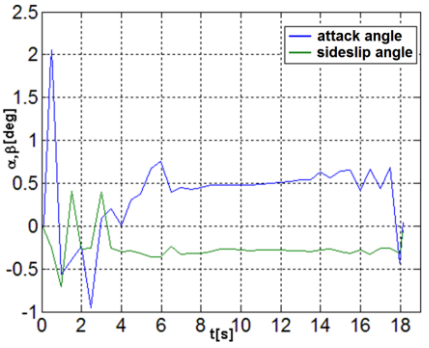

Fig. 20. Attack and sideslip angles

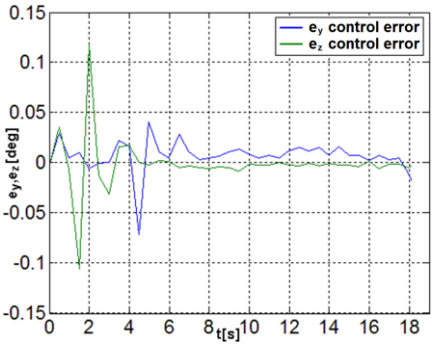

Fig. 21. Control errors

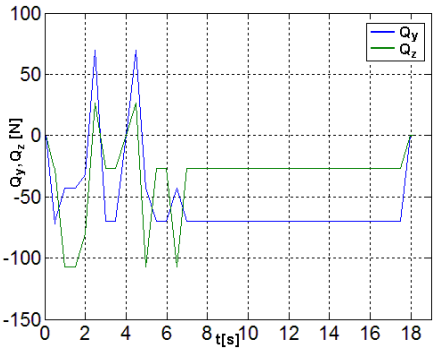

Fig. 22. Control force values

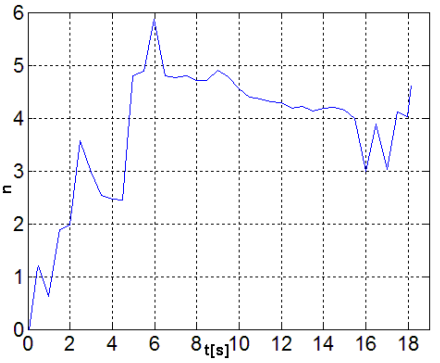

Fig. 23. Kinematic g-loads

5. CONCLUSION

The analysis of the simulation test results provided the following conclusions:

- The application of the method proposed herein and based on phase trajectories of control errors for guidance of the SAM to an airborne target was feasible and realistic.
- The SAM's target hit accuracy for a target of 6.25 m in length during the FH attack and for a target of 5.90 m in length during the AH attack was sufficient for the SAM's effectiveness, especially if the SAM was equipped with a proximity detonator.
- Both in the FH and AH attacks, the task of hitting a moving airborne target was fulfilled.
- The control forces in both analysed cases reached low values, which were feasible for implementation in real-world conditions [14].
- In a similar fashion, the attack and sideslip angles also reached low values.

- The g-load applied to the SAM in mid-flight were acceptable, with a maximum limit of approximately 15 g.
- The slight oscillations of the actual realised flight path of the SAM were a result of function sgn applied to control the SAM.
- In the future, an attempt should be made at implementing this method to control the homing of a SAM with more complex manoeuvring of its airborne target.
- It is prudent to attempt an analysis of the same control method applied in an anti-tank guided missile.

REFERENCES

[1] Hsu C. Jay, Andrew U. Meyer. 1968. *Modern control principles and application.* McGraw-Hill, New York.

[2] Osiecki W. Jan, Konrad Stefański. 2008. "On a method of target detection and tracking used in air defence". *Journal of Theoretical and Applied Mechanics* 46 (4): 909-916.

[3] Baranowski Leszek, Bogdan Machowski. 2011. "The analysis of efficiency of proportional navigation method in gas-dynamic control of spinning objects in flight" (in Polish). *Problemy mechatroniki. Uzbrojenie, lotnictwo, inżynieria bezpieczeństwa – Problems of Mechatronics. Armament, Aviation, Safety Engineering* 1(3): 37-54.

[4] Koruba Zbigniew, Edyta Ładyżyńska-Kozdraś. 2010. "The dynamic model of a combat target homing system of an unmanned aerial vehicle". *Journal of Theoretical and Applied Mechanics* 48(3): 551-566.

[5] Krzysztofik Izabela. 2012. „The dynamics of the controlled observation and tracking head located on a moving vehicle". *Solid State Phenomena* 180: 313-322.

[6] Gapiński Daniel, Zbigniew Koruba, Izabela Krzysztofik. 2014. "The model of dynamics and control of modified optical scanning seeker in anti-aircraft rocket missile". *Mechanical Systems and Signal Processing* 45(4): 433-447.

[7] Gapiński Daniel, Konrad Stefański. 2014. "Control of designer target seeker used in self-guided anti-aircraft missiles, by employing motors with a constant torque". *Aviation* 18(1): 20-29.

[8] Koruba Zbigniew, Łukasz Nocoń. 2015. "Automatic control of an anti-tank guided missile based on polinomial functions". *Journal of Theoretical and Applied Mechanics* 53(1): 139-150.

[9] Grzyb Marta, Konrad Stefański. 2016. The use of special algorithm to control the flight of anti-aircraft missile. W *Proceedings of the 22nd International Conference Engineering Mechanics, Svratka, Czech Republic*: 174-177. Academy of Science of the Czech Republic, Prague.
[10] Koruba Zbigniew, Jan W. Osiecki. 1999. *Constructions, dynamics and navigation of the short range rocket missile* (in Polish). 1st part, Academy Course Book, 348. Kielce: Kielce University of Technology.
[11] Koruba Zbigniew, Janusz Tuśnio. 2011. "Concept and algorithm of flying object protection manoeuvre against collision with overhead high voltage transmission line" (in Polish). *Problemy mechatroniki. Uzbrojenie, lotnictwo, inżynieria bezpieczeństwa – Problems of Mechatronics. Armament, Aviation, Safety Engineering* 4(6): 69-80.
[12] Yanushevsky Rafael. 2011. *Guidance of unmanned aerial vehicles*. New York: Taylor & Francis Group.
[13] Stefański Konrad, Marta Grzyb. 2013. "Comparison of effectiveness of antiaircraft missile homing controlled by rotary executive system" (in Polish). *Problemy mechatroniki. Uzbrojenie, lotnictwo, inżynieria bezpieczeństwa – Problems of Mechatronics. Armament, Aviation, Safety Engineering* 4(14): 27-40.
[14] Dziopa Zbigniew. 2013. „"The evaluation of the defensive maneuvers influence on the missile control" (in Polish). *Scientific Letters of Rzeszow University of Technology* no. 288, *Mechanics* no. 85, XXX (3/13) : 229-238.

Zastosowanie specjalnego sposobu wyznaczania sił sterujących do realizacji samonaprowadzania na cel powietrzny przeciwlotniczego pocisku rakietowego z wykorzystaniem metody proporcjonalnej nawigacji

Konrad STEFAŃSKI

Politechnika Świętokrzyska, Wydział Mechatroniki i Budowy Maszyn
al. Tysiąclecia Państwa Polskiego 7, 25-314 Kielce

Streszczenie. W pracy przeprowadzono analizę możliwości zastosowania specjalnej metody sterowania przeciwlotniczym pociskiem rakietowym podczas naprowadzania na ruchomy cel powietrzny. Wcześniej w oparciu o tę metodę zrealizowane zostało sterowanie ruchem osi giroskopu o trzech stopniach swobody [1, 2] w czasie przeszukiwania przestrzeni i śledzenia wykrytego celu. Otrzymane wtedy pozytywne wyniki dały podstawę do wyciągnięcia wniosku, że zaproponowane sterowanie będzie możliwe do wyznaczania sił sterujących przy naprowadzaniu pocisku rakietowego. Metoda ta polega na wykorzystaniu trajektorii fazowych uchybów sterowania. Przełączanie sił sterujących w odpowiednich punktach płaszczyzny fazowej powoduje sprowadzanie tych uchybów do zera i realizację odpowiedniego toru lotu pocisku rakietowego. Zaprezentowano algorytm przełączania, równania kinematyki i dynamiki lotu pocisku oraz wiele przykładów symulacji numerycznych. Otrzymane wyniki zostały przedstawione w postaci graficznej.
Słowa kluczowe: mechanika, sterowanie, trajektorie fazowe, samonaprowadzanie, cel